

**DESIGN OF IMPEDANCE MATCHING NETWORKS
FOR A RECTANGULAR PATCH ANTENNA**

J.W. Bandler, N. Georgieva and F. Guo

SOS-00-20-R

June 2000

© J.W. Bandler, N. Georgieva and F. Guo 2000

No part of this document may be copied, translated, transcribed or entered in any form into any machine without written permission. Address inquiries in this regard to Dr. J.W. Bandler. Excerpts may be quoted for scholarly purposes with full acknowledgment of source. This document may not be lent or circulated without this title page and its original cover.

DESIGN OF IMPEDANCE MATCHING NETWORKS FOR A RECTANGULAR PATCH ANTENNA

J.W. Bandler, N. Georgieva and F. Guo

Simulation Optimization Systems Research Laboratory
and Department of Electrical and Computer Engineering
McMaster University, Hamilton, Canada L8S 4K1

Tel 905 628 9671 Fax 905 628 1578 Email j.bandler@ieee.org

Abstract

The narrow bandwidth is probably the most serious problem that restricts the development of patch antennas. Impedance matching network technique [1] is a possible way to elevate the drawback. In this report, the design procedure proposed in [1] is followed. The impedance matching network consisting of open stubs and quarter-wavelength transformers is obtained. In order to reduce distortion of far field pattern brought about by electromagnetic coupling between the impedance matching network and the patch antenna, an alternative impedance matching network is proposed and the design procedure is given. It is implemented by parallel-coupled microstrip lines. The simulation results show it decreases the distortion of the far field pattern. All of these designs are carried out using *OSA90/hope*TM [2]. The final designs are verified by the EM simulator MomentumTM [3].

I. INTRODUCTION

The inherent narrow bandwidth is one of the serious problems that impede the application of microstrip antennas in many systems [4]. Experimental investigation clearly shows that the impedance variations are the dominant bandwidth-limiting factor, whereas the gain and radiation pattern variations

This work was supported in part by the Natural Sciences and Engineering Research Council of Canada under Grants OGP0007239 and STP0201832, and through the Micronet Network of Centres of Excellence.

J.W. Bandler and F. Guo are with the Simulation Optimization Systems Research Laboratory and the Department of Electrical and Computer Engineering, McMaster University, Hamilton, Ontario, Canada, L8S 4K1.

N. Georgieva are with the Department of Electrical and Computer Engineering, McMaster University, Hamilton, Ontario, Canada, L8S 4K1.

J.W. Bandler is also with Bandler Corporation, P.O. Box 8083, Dundas, Ontario, Canada L9H 5E7.

are almost negligible over a moderate 10 to 20 percent bandwidth [1]. The phenomena can be explained by the theory of modal expansion in a cavity. It has been applied in the cavity model analysis of microstrip antennas [1]. On the basis of these facts, a broadband impedance matching technique is proposed in [1] as a method for bandwidth enhancement of microstrip antennas.

Design of a broadband impedance matching network is a difficult network synthesis problem. It is always a kind of trade-off between increased bandwidth and degree of matching. It was limited by Bode-Fano criteria [5]. Some efficient design techniques could be found in [6]. These procedures assume that the load to be matched can be approximated over the frequency band of interest by a simple RLC resonant circuit. The design result depends partly on how closely the load to be matched resembles a simple RLC circuit within the frequency range of interest.

The example in [1] is considered and the design result is reproduced by following the design procedure proposed in the paper. The result is verified by MomentumTM and discussed in the Appendix. EM simulation result shows that the resultant impedance matching network distorts the far field pattern of the patch antenna because of strong electromagnetic coupling between the patch and the impedance matching network. In Section II, an alternative design procedure is given to reduce the distortion of the far field pattern. According to the proposed design procedure, the parallel-coupled line form of impedance matching network is achieved in Section II. The initial design is optimized using *OSA90/hope*TM and then the optimal design is verified by MomentumTM. In Section III, the analysis of EM simulation results is carried out by decomposing the whole structure into two parts, that is, the radiator and the impedance matching network. Finally, the conclusions are given in Section IV.

II. DESIGN PROCEDURE OF THE IMPEDANCE MATCHING NETWORK

A. Characterization of the Patch Antenna

As shown in Fig. 1, the patch antenna to be matched is a rectangular patch antenna (RPA). The width W_0 is 120mm and length L_0 is 31.5mm. The patch is mounted on a substrate whose thickness h is 1.60mm and relative permittivity ϵ_r is 2.20. The return loss versus frequency is plotted in Fig. 2a. The

input impedance of the RPA can be calculated from the transmission line model [7]. It is shown in Fig. 2b. Fig. 2c and Fig. 2d show the real and imaginary part of the impedance of the RPA, respectively. Fig. 2e and Fig. 2f show the real and imaginary part of the admittance of the RPA, respectively. They are very typical plots of the electrical characteristics of microstrip antennas.

As we know, the impedance matching network technique [6] is based on the assumption that the load to be matched can be approximated by a simple RLC circuit. In comparison with the impedance versus frequency plot, the admittance versus frequency plot behaves more like a parallel resonant RLC circuit. However, as mentioned in the Appendix, the matching network consisting of open stubs and quarter wavelength transmission lines affects the far field pattern of the RPA severely.

A good way to solve the problem is to use a parallel-coupled transmission line impedance matching network. Meanwhile, an additional quarter wavelength transmission line is needed to separate the matching network from the RPA. The characteristic impedance of the additional transmission line is equal to the resonant resistance of the RPA. The transmission line is a quarter wavelength transformer at the resonant frequency of the RPA. Then, the impedance of the radiator (RPA+quarter wavelength transformer) behaves more like a series resonant RLC circuit over a certain frequency band (from 2.9GHz to 3.1GHz) instead of a parallel resonant RLC circuit. It is shown in Fig. 3. Fig. 3a shows the real part of the impedance of the radiator. Fig. 3b shows the imaginary part of the impedance of the radiator. These results are achieved using the transmission line model [7] implemented by *OSA90/hope*TM.

Once the impedance plot is given, the resonant quality factor of the radiator can be computed by

$$Q = \frac{x_1}{R_A} \quad (1)$$

where R_A is the approximate resistance over the frequency band of interest and x_1 is the reactance slope parameter given by

$$x_1 = \frac{\omega_0}{2} \left. \frac{dX}{d\omega} \right|_{\omega_0} \quad (2)$$

where X is the reactance of the radiator and ω_0 is the resonant frequency. After some simple calculations, the resonant resistor R_A and reactance slope x_1 can be obtained from Fig. 3a and Fig. 3b. In the problem considered in this report, the resonant quality factor Q is 46.265. The result is obtained using the transmission line model of the radiator. It is different from the result given by measurement in [1].

The additional quarter wavelength transformer has two main functions. One is to separate the RPA from the impedance matching network, the other is the transformation of the impedance of the RPA.

The relative bandwidth of the radiator can be obtained directly from the plot of return loss versus frequency (Fig. 2a) or by

$$W = \frac{1}{Q} \sqrt{\frac{(TS-1)(S-T)}{S}} \quad (3)$$

where $T=Z_0/R_0$ in the series-resonant case, the bandwidth criterion is taken to be $VSWR \leq S$ which is set equal to 2. It means that the return loss is less than about -10 dB within the passband. The maximum impedance bandwidth [1] is given in (4). In this case, it is equal to 6.18%.

$$W_m = \frac{1}{Q} \frac{\pi}{\ln[(S+1)/(S-1)]} \quad (4)$$

B. Design Procedure of the Impedance Matching Network

The impedance matching network design technique was developed on the basis of the band-pass microwave filter design theory [6]. The basic idea behind the design technique is that the radiator can be considered as the first resonator of the corresponding microwave filter.

As mentioned in part A of this section, the radiator can be approximated by a series resonant RLC circuit. After parameters of the lumped circuit are determined, an appropriate form of impedance matching network will be chosen. Since the impedance matching network proposed in [1] would affect the far field pattern, the parallel-coupled transmission line form is adopted in place of the impedance matching network consisting of open stubs connected by quarter wavelength transmission lines. The prototype of the impedance matching network is shown in Fig. 4. Detailed design steps are given below.

Step 1. The order of the matching network n is chosen according to the decrement [6]

$$\delta = \frac{1}{WQ} \quad (3)$$

where W is determined a priori according to the W_m . In this case, n is chosen to be 3.

Step 2. Knowing n and δ , the g_i parameters ($i=2, 3$) are found from [6], the parallel-coupled transmission line prototype is taken as the impedance matching network. The corresponding parameters are determined by the following equations given in [6], [8] and [9].

$$\frac{J_{12}}{Y_0} = \frac{1}{\omega'_{1}} \sqrt{\frac{\pi W G_A}{2Y_0 g_1 g_2}} \quad (4)$$

$$\frac{J_{k,k+1}}{Y_0} = \frac{\pi W}{2\omega'_{1}} \frac{1}{\sqrt{g_k g_{k+1}}}, \quad k = 2 \text{ to } n-1 \quad (5)$$

$$\frac{J_{n,n+1}}{Y_0} = \sqrt{\frac{\pi W}{2g_n g_{n+1} \omega'_{1}}} \quad (6)$$

where $\omega'_{1}=1$ in this report, Y_0 is set equal to 50Ω .

The even- and odd- mode impedances of the strips are

$$(Z_{0e})_{j,j+1} \Big|_{j=1 \text{ ton}} = \frac{1}{Y_0} \left[1 + \frac{J_{j,j+1}}{Y_0} + \left(\frac{J_{j,j+1}}{Y_0} \right)^2 \right] \quad (7)$$

$$(Z_{0o})_{j,j+1} \Big|_{j=1 \text{ ton}} = \frac{1}{Y_0} \left[1 - \frac{J_{j,j+1}}{Y_0} + \left(\frac{J_{j,j+1}}{Y_0} \right)^2 \right] \quad (8)$$

Step 3. Once the even-mode and odd-mode impedances are given, the practical geometry dimensions of corresponding parallel-coupled transmission lines fabricated on the substrate are determined using some empirical formulas in [10]. However, it should be mentioned that these formulas are not accurate enough. In order to avoid lengthy trail-and-error tuning procedures, the final design relies on the optimization technique. In this report, *OSA90/hope*TM is used to optimize the initial design. The optimization specifications are

$$|S_{11}| \geq -3.0\text{dB} \quad 2.70\text{GHz} \leq f \leq 2.85\text{GHz} \quad (9)$$

$$\begin{aligned} |S_{11}| &\leq -10\text{dB} & 2.90\text{GHz} \leq f \leq 3.10\text{GHz} & (10) \\ |S_{11}| &\geq -3.0\text{dB} & 3.15\text{GHz} \leq f \leq 3.30\text{GHz} & (11) \end{aligned}$$

In order to get a good result, the minimax optimization method is utilized.

III. EM SIMULATION AND RESULTS ANALYSIS

Following the steps in Section II, the optimal design based on the circuit simulator is achieved. The layout of the impedance matching network is shown in Fig. 5. The return loss of the antenna before matching is shown in Fig. 6a. Fig. 6b is the return loss of the optimal design. The optimal parameters are listed in Table I. Since the optimal design is obtained on the basis of the circuit simulator, it should be verified by EM simulation. In this report, MomentumTM is used to verify the circuit simulator based optimal design. The EM simulation result is shown in Fig. 6c. It is different from the optimal response obtained by the circuit simulator. Obviously, the circuit simulator based model is very coarse.

In order to find the reason that leads to the difference, the whole structure is decomposed into two parts. One is the radiator, the other is the matching network. Fig. 7a is the circuit simulation result of the radiator, whereas Fig. 7b is the EM simulation result. It shows that the result given by the transmission line model is close to the EM simulation result over the frequency band of interest (2.7GHz – 3.3GHz). However, in comparison with the EM simulation result of the impedance matching network, the circuit simulation result has a big shift and an amplitude deformation. The geometry of the impedance matching network is shown in Fig. 8. The scattering parameters versus frequency plots are shown in Fig. 9a and Fig. 9b. Fig. 9a is the EM simulation result and Fig. 9b is the circuit simulation result.

In comparison with the far field pattern of the antenna matched by the matching network proposed in [1], the far field pattern of the antenna, which is matched by the matching network proposed in the report, looks more like that of the antenna before matching. It is shown in Fig. 10. In other words, the impedance matching network proposed in this report has less effect on the far field pattern. In order to reduce the distortion, a shielding cover was added on the top of the matching network proposed in [1].

IV. CONCLUSIONS

The circuit simulation results show that the impedance-matching network can enhance the bandwidth of the RPA. But the maximum bandwidth depends on the acceptable return loss criterion as well as the resonant quality factor Q of the RPA.

The electromagnetic simulation results show that the proposed impedance matching network has less effect on the far field pattern than that proposed in [1]. On the other hand, the circuit simulator based design must be improved by the optimization technique integrated with EM simulation. The quality factor Q and resonant resistance R_A of the RPA are calculated from the circuit simulation result. They are close to the result obtained from the EM simulation. However, the EM simulation result is different from the circuit simulation result of the impedance matching network part.

REFERENCES

- [1] H.F. Pues and A.R. Van De Capelle, "An impedance-matching technique for increasing the bandwidth of microstrip antennas," *IEEE Trans. Antennas Propagation*, vol. AP-37, 1989, pp. 1345-1354.
- [2] *OSA90/hope*TM Version 4.0, formerly Optimization Systems Associates Inc., P.O. Box 8083, Dundas, Ontario, Canada L9H 5E7, now Agilent Technologies, 1400 Fountaingrove, Parkway, Santa Rosa, CA 95403-1799.
- [3] *Momentum*TM Version 3.0, Agilent Technologies, 1400 Fountaingrove Parkway, Santa Rosa, CA 95403-1799, 1998.
- [4] D.M. Pozar and D.H. Schubert, *Microstrip Antennas: The Analysis and Design of Microstrip Antennas and Arrays*. New York: IEEE Press, 1995.
- [5] D.M. Pozar, *Microwave Engineering*. New York: Addison Wesley, 1990.
- [6] G.L. Matthaei, L. Young and E.M. T. Jones, *Microwave Filters, Impedance-Matching Network and Coupling Structures*. New York: McGraw-Hill, First Edition, 1964.
- [7] J.W. Bandler, M.H. Bakr and N.Georgieva, "A space mapping model for microstrip rectangular patch antennas," SOS-99-17-R, June 1999.
- [8] S.B. Cohn, "Parallel-coupled transmission-line-resonator filters," *IRE Trans. Microwave Theory Tech.*, vol. 6, 1958, pp. 223-231.
- [9] S.B. Cohn, "Direct-coupled-resonator filters," *Proc. IRE*, vol. 45, 1957, pp. 187-196.

[10] T.C. Edwards, *Foundations for Microstrip Circuit Design*. New York: John Wiley & Sons, 1981.

APPENDIX

THE IMPEDANCE MATCHING NETWORK PROPOSED IN [1]

Following the design procedure reported in [1], the matching network prototype consisting of open stubs and quarter wavelength transformers is achieved. The layout of the impedance matching network is shown in Fig. 11. The return loss of the antenna before matching is shown in Fig. 12a. The initial design is optimized using the minimax optimizer in *OSA90/hope*TM. The return loss of the impedance of the matched antenna is shown in Fig. 12b. The optimal parameters of the matching network are given in Table II. The optimal design is verified by the EM simulator MomentumTM. The result is shown in Fig. 12c.

Since the open stubs are very wide and close to the RPA, the electromagnetic coupling between them distorts the far field pattern seriously. It is shown in Fig. 10. Fig. 10a is the far field pattern of the rectangular patch antenna. Fig. 10b is the far field pattern of the antenna matched by the open stub form of impedance matching network. Fig.10c is the far field pattern of the antenna matched by the parallel-coupled transmission line form of impedance matching network. It can be seen that the impedance matching network proposed in this report decreases the distortion of the far field pattern.

TABLE I
THE OPTIMAL DESIGN OF THE IMPEDANCE MATCHING
NETWORK PROPOSED IN THIS REPORT

Parameter	Value	Parameter	Value
L_0	31.500	W_0	120.00
L_1	18.117	W_1	4.7464
L_2	19.146	W_2	4.2768
L_3	16.519	W_3	8.7157
L_4	19.259	W_4	4.8093
S_1	0.1402	S_2	0.8139
S_3	0.0847		
Values are in millimeters			

TABLE II
THE OPTIMAL DESIGN OF THE IMPEDANCE MATCHING
NETWORK PROPOSED IN [1]

Parameter	Value	Parameter	Value
L_0	31.500	W_0	120.00
L_1	18.099	W_1	2.9811
L_2	18.454	W_2	1.0910
L_3	18.191	W_3	3.1077
L_4	35.355	W_4	11.568
Values are in millimeters			

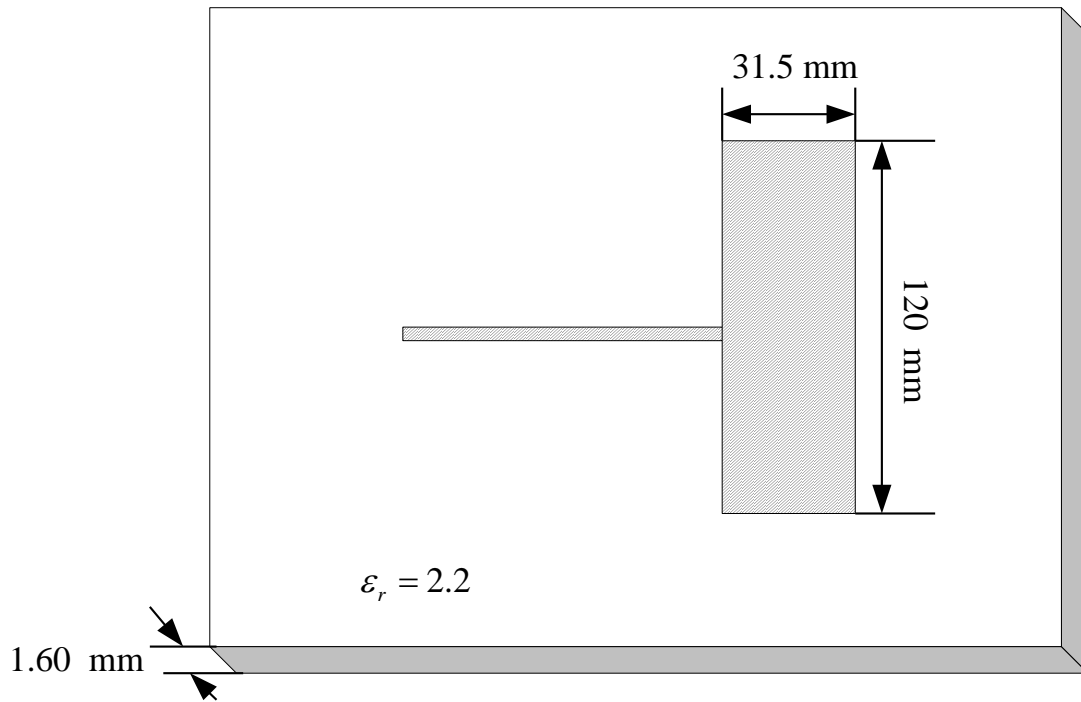
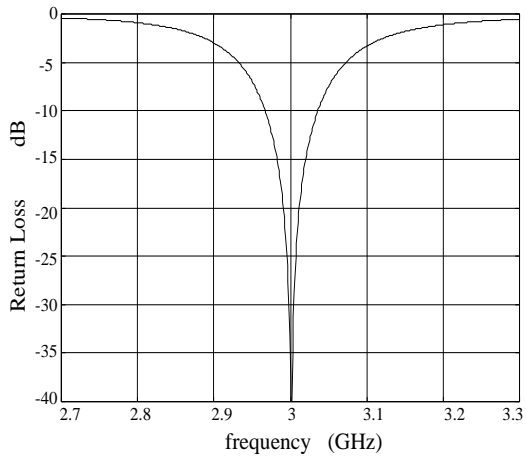
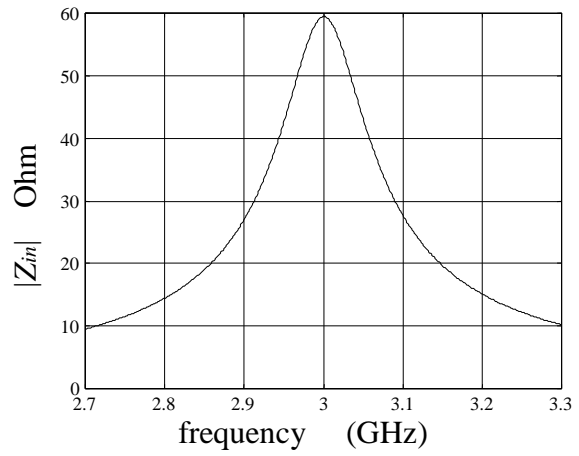


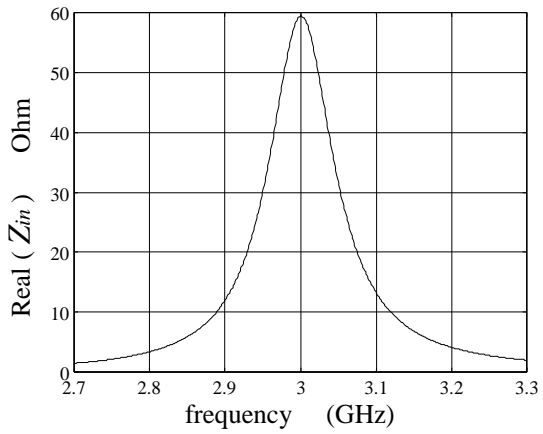
Fig. 1. The geometry of the patch antenna to be matched.



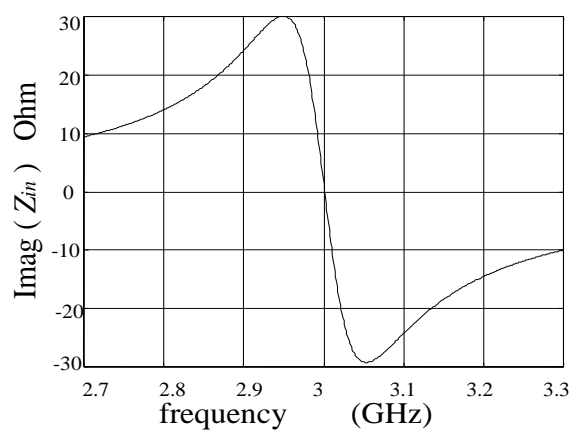
(a)



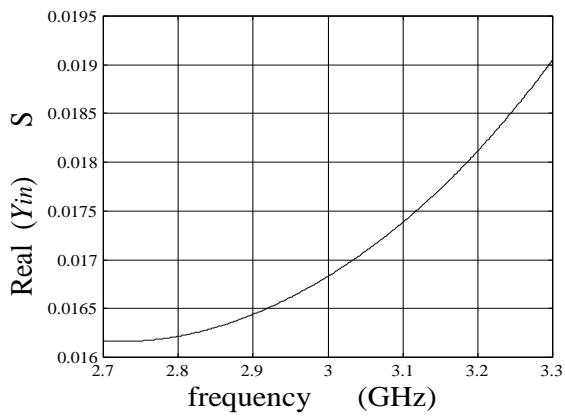
(b)



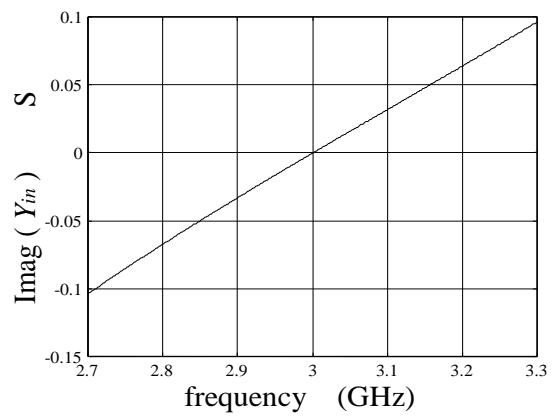
(c)



(d)

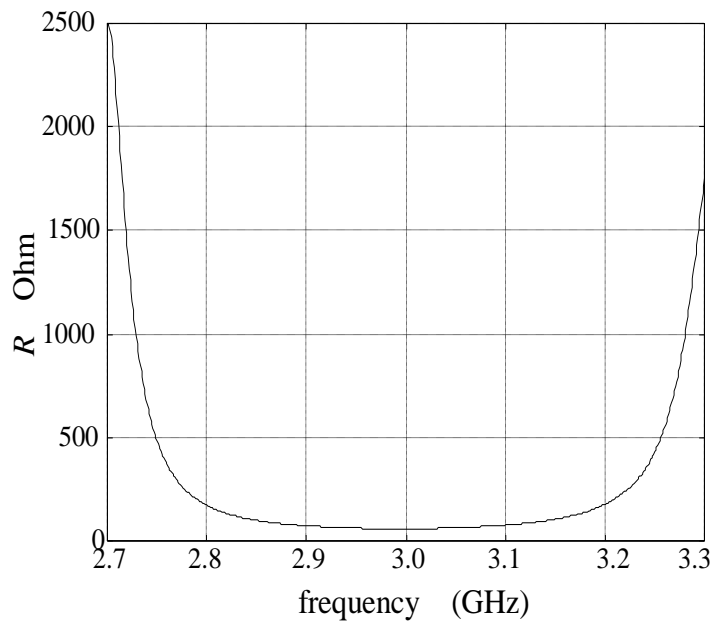


(e)

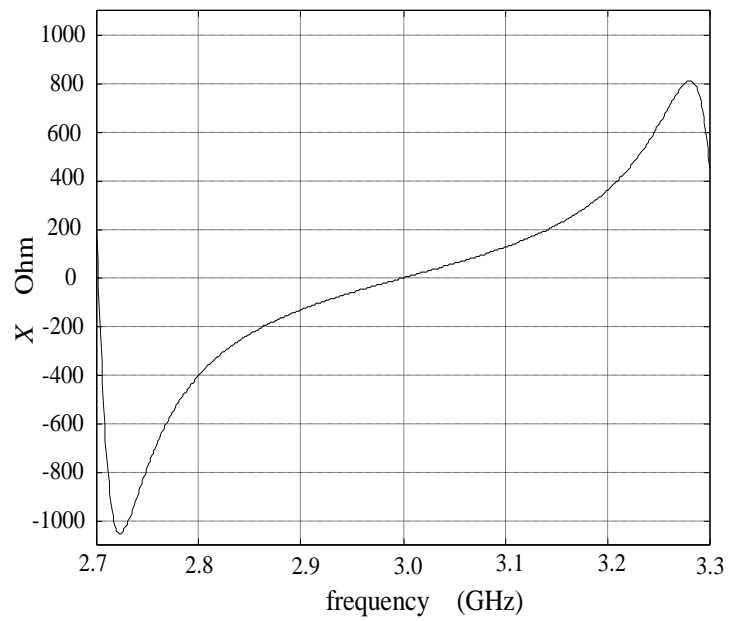


(f)

Fig. 2. Some electrical characteristics of the patch antenna to be matched: (a) the return loss of the RPA, (b) the input impedance of the RPA, (c) the real part of the impedance of the RPA, (d) the imaginary part of the impedance of the RPA, (e) the real part of the admittance of the RPA, (f) the imaginary part of the admittance of the RPA.



(a)



(b)

Fig. 3. The real and imaginary part of the impedance of the radiator: (a) the real part of the input impedance, (b) the imaginary part of the input impedance.

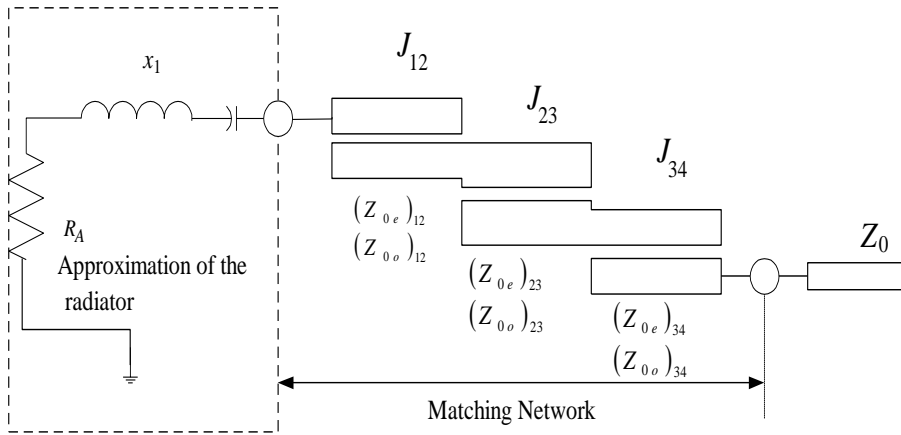


Fig. 4. The coupled transmission line prototype of the impedance matching network.

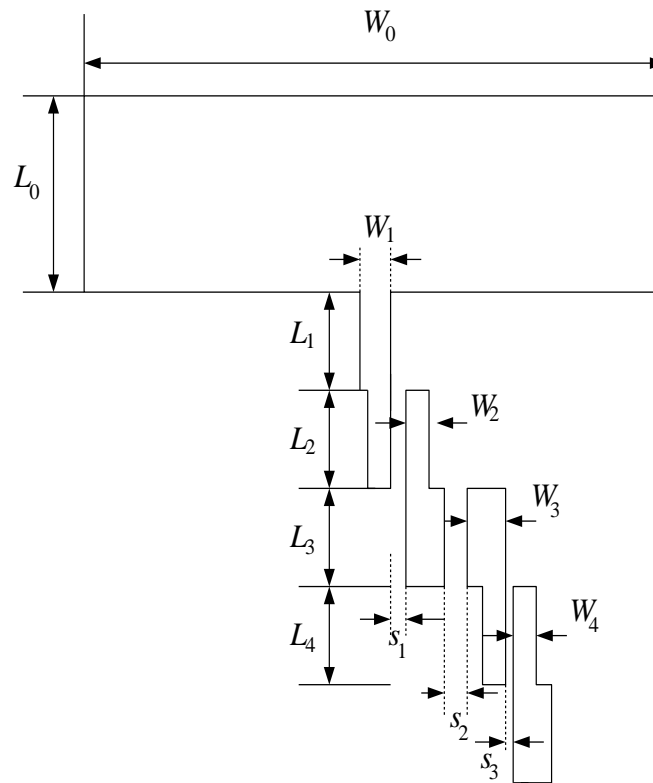
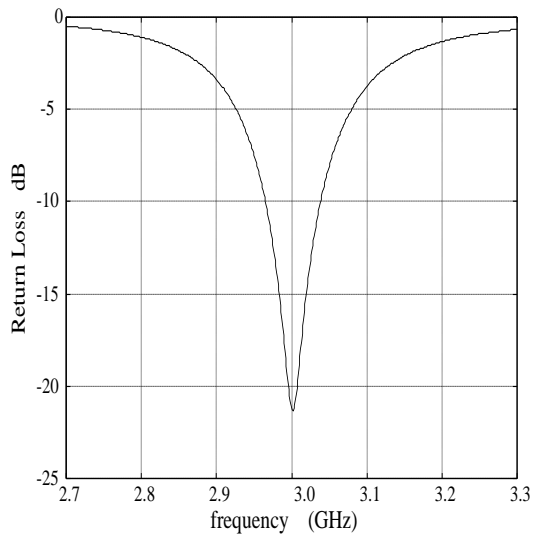
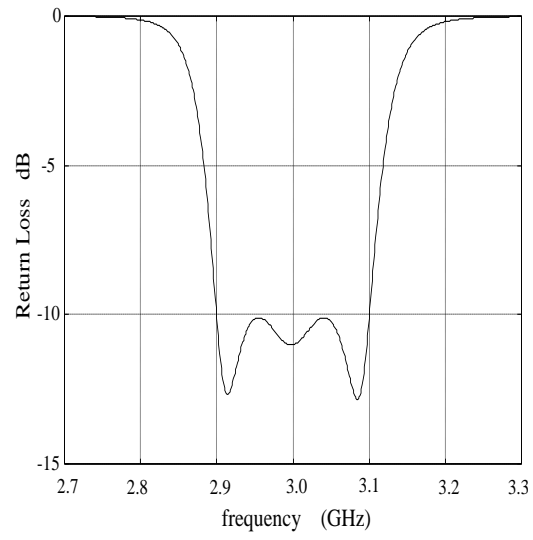


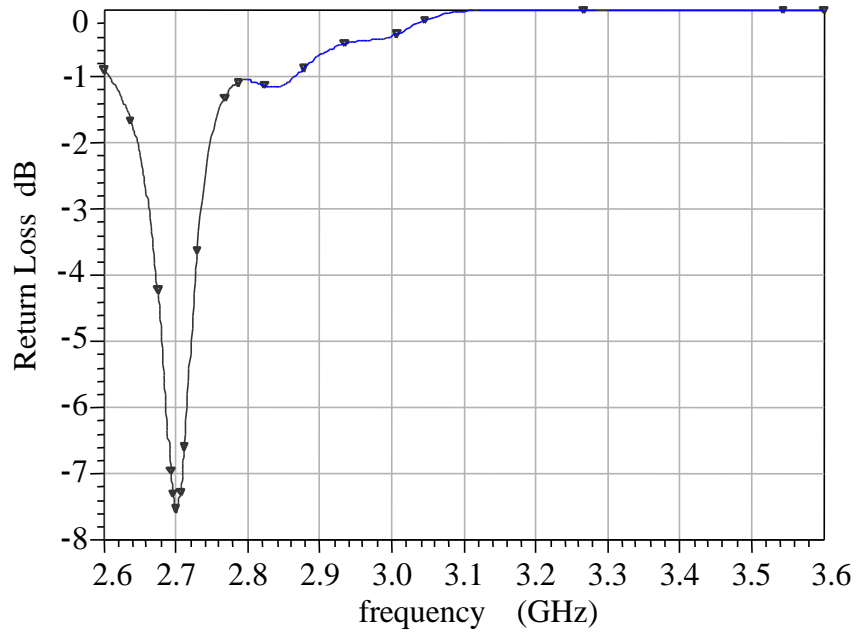
Fig. 5. The geometry of the parallel-coupled transmission line impedance matching network.



(a)

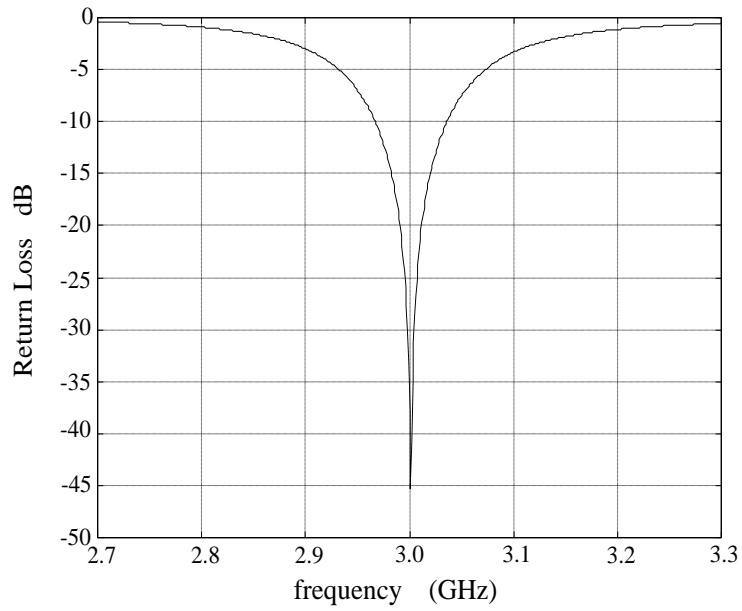


(b)

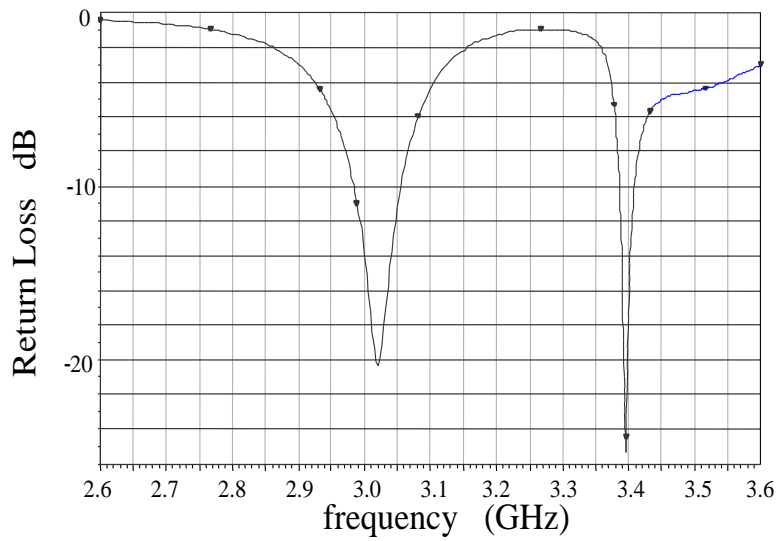


(c)

Fig. 6. The return loss comparison: (a) the return loss of the antenna before matching (result obtained from *OSA90/hope*TM), (b) the return loss of the antenna after matching by the parallel coupled microstrip line form of impedance matching network (result obtained from *OSA90/hope*TM), (c) the return loss of the EM model (result obtained from *Momentum*TM).



(a)



(b)

Fig. 7. Comparison between the EM model and empirical model of the radiator: (a) the result obtained from MomentumTM, (b) the result obtained from OSA90/hopeTM.

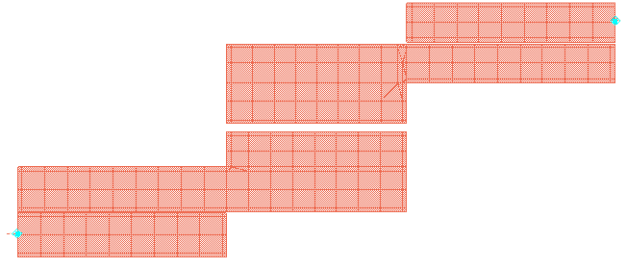
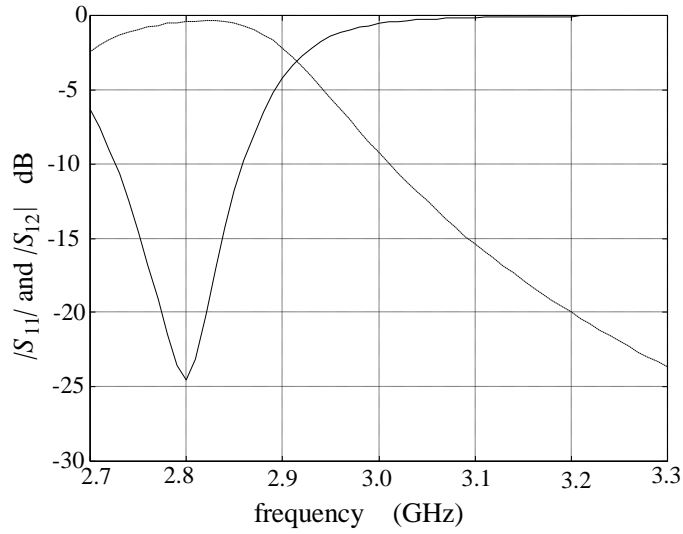
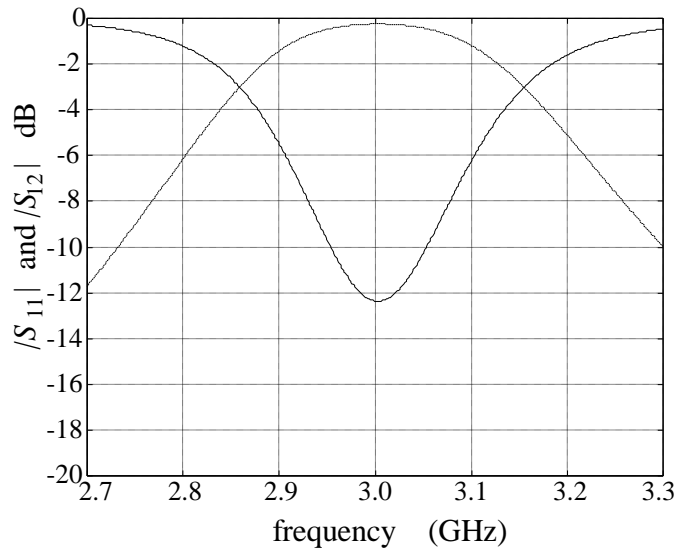


Fig. 8. The geometry of the impedance matching network.



(b)



(c)

Fig. 9. Comparison between the EM model and the equivalent circuit model of the impedance matching network ($|S_{11}|$ dB (—) and $|S_{12}|$ dB (---)): (a) the result obtained from MomentumTM, (b) the result obtained from OSA90/hopeTM.

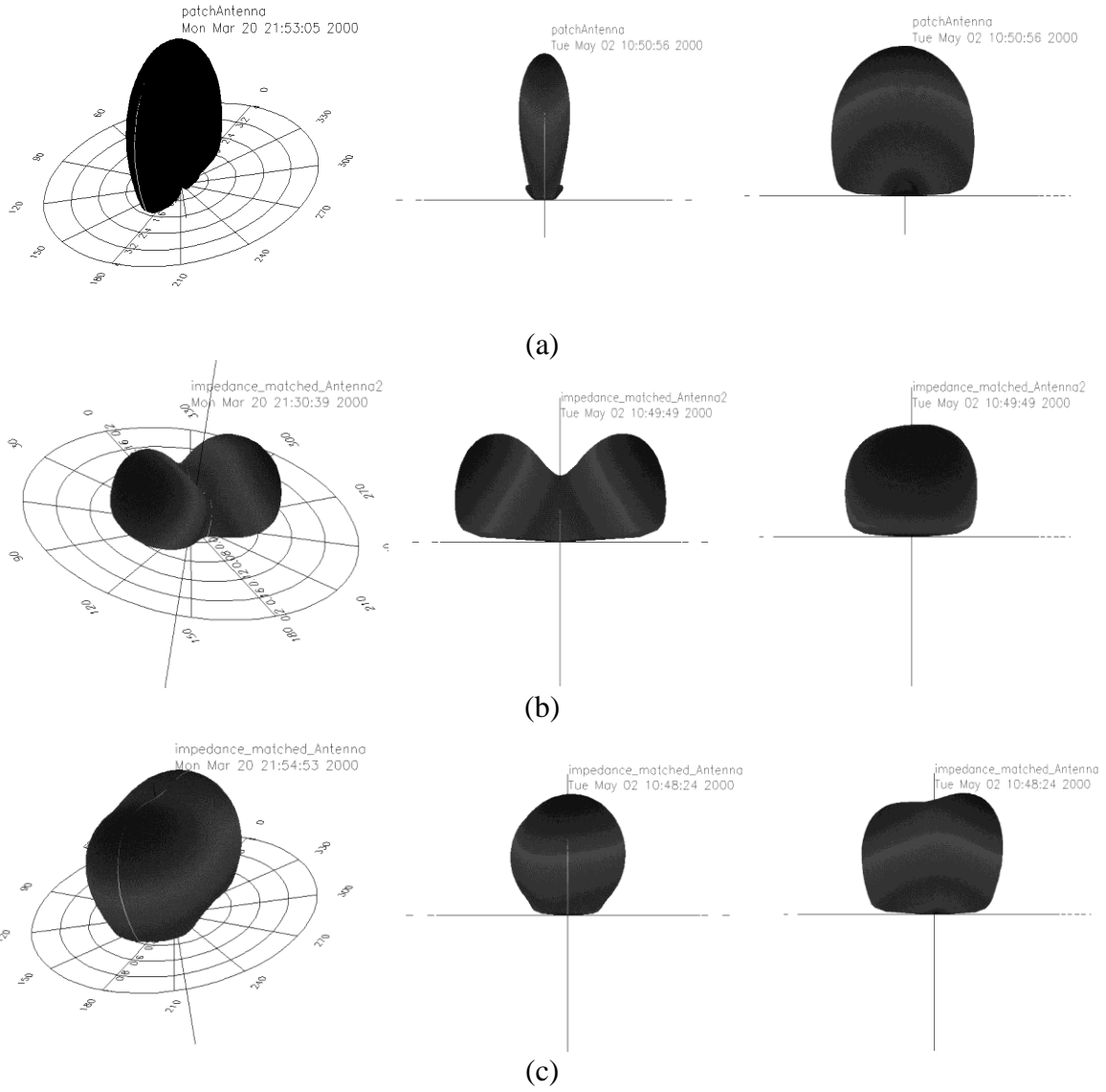


Fig. 10. The comparison of the far field patterns (computed at 2.6GHz): (a) far field pattern, front view and side view of the far field pattern of the reference antenna, (b) far field pattern, front view and side view of the far field pattern of the antenna matched by the open stub form of impedance matching network, (c) far field pattern, front view and side view of the far field pattern of the antenna matched by the coupled transmission line form of impedance matching network.

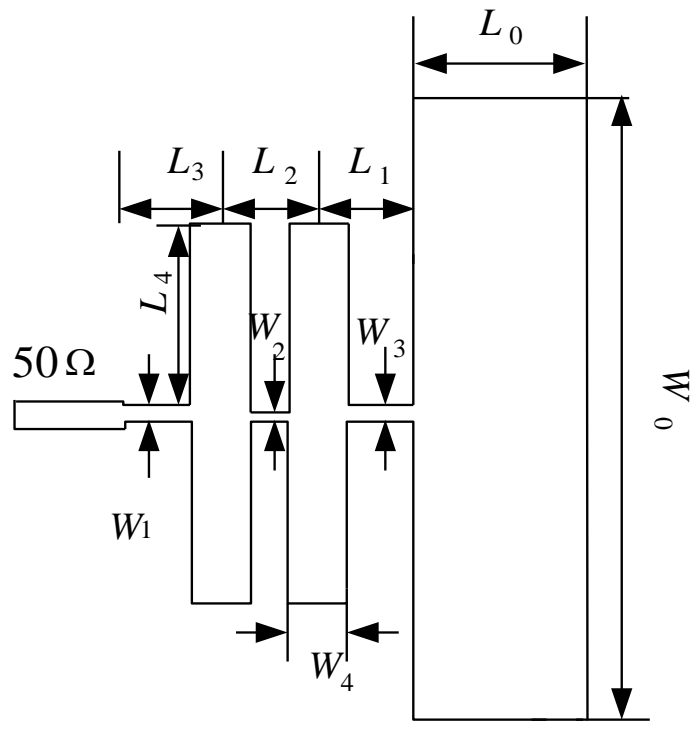


Fig. 11. The geometry of the open stub form of impedance matching network.

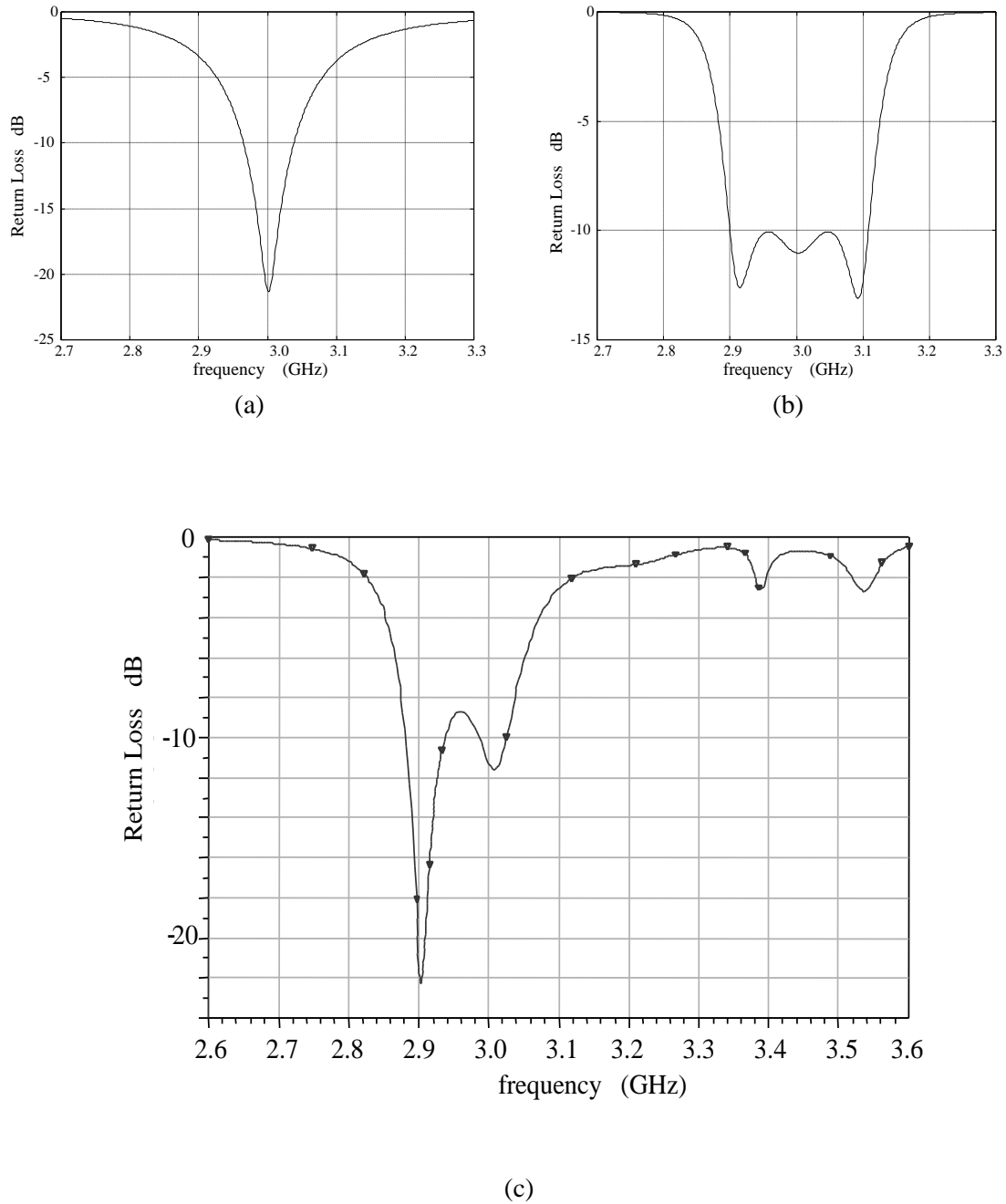


Fig. 12. The return loss comparison: (a) the return loss of the antenna before matching (result obtained from *OSA90/hope*TM), (b) the return loss of the antenna after matching by the open stub form of impedance matching network (result obtained from *OSA90/hope*TM), (c) the return loss of the EM model (result obtained from *Momentum*TM).